ENHANCEMENT OF MODE I FRACTURE TOUGHNESS OF ADHESIVELY BONDED SECONDARY JOINTS USING LAYUP PATTERNING OF CFRP

R. A. A. Lima [a], A. Oswal [c], N. Roux [b], A. Bernasconi [a], M. Carboni [a], N. Carrere [c], S. Teixeira de Freitas [b]

[a] Department of Mechanical Engineering, Politecnico di Milano – Milan, Italy

[b] Faculty of Aerospace Engineering, Delft University of Technology – Delft, Netherlands

[c] ENSTA Bretagne, UMR CNRS 6027, IRDL, F-29200 – Brest, France

Abstract: *This work aims to analyse the influence of the CFRP layup patterning on the crack path of composite bonded joints and evaluate its effect on the mode I fracture toughness. An experimental program has been performed using Double Cantilever Beam tests with three different CFRP layup patterning and two adhesives. In addition, a finite element analysis was also implemented to further identify different damage mechanisms during the tests.*
The outcome shows that different substrate CFRP layup patterning results in distinct crack onsets and propagation paths during the tests, also influenced by the type of adhesive used. Furthermore, an enhancement of around 25% in the joint's onset fracture toughness was observed with the layup patterning compared to a reference joint (with unidirectional layup). Thus, the substrate's patterning morphology seems to be a promising method to increase the mode I fracture toughness of the studied secondary joints.

Keywords: CFRP patterning layups, fracture toughness, secondary bonded joints.

1. Introduction

Recently, with a worldwide demand to promote eco-friendly solutions to several industrial processes and products, the automotive and aeronautical sectors aim for lightweight structures. Consequently, multi-advanced materials such as new-modified steel alloys and composite materials are increasingly being used [1]. Adhesive joining technology is one of the most promising solutions to join multi-materials, especially composites, as it brings design flexibility, uniform stress distribution, and a limited impact on substrates' mechanical performance compared to traditional fasteners.

Nevertheless, adhesively bonded joints face challenges in ensuring reliability and safety during their operational life, as they tend to fail suddenly and show a limited tolerance to damage [2]. Consequently, to prevent catastrophic failure in safety-critical bonded joints, "back-up" rivets are used in current composite primary structures.

One promising solution to improve the reliability and safety of secondary bonded joints in primary structures is to enhance the joint's damage resistance and fracture toughness [3]. Different methods have been proposed in the literature to increase the fracture toughness of composite bonded joints: improving the adhesive's mechanical properties by modifications in the adhesive layer [4]; introducing Crack stoppers within the adhesive layer [5] [6]; interfacial

adhesion patterning over substrate's surface [7] [8]; and tailor the composite's stacking sequences [9][10].

Kupski *et al*. 2019 [11] investigated the effects of different stacking sequences and plies thickness on the mechanical behaviour of Single-Lap Joints (SLJ). It was observed that the crack propagates through different layers inside the composite when using a thin ply thickness instead of persuing single in-plane delamination when using a thicker ply thickness. As a result, multiple transverse matrix cracking co-occurs, increasing the energy dissipation and enhancing the SLJ strength for damage initiation.

Nonetheless, it is still unclear which mechanisms trigger the changes in the damage resistance of the SLJ due to their complex stress state. In the pursue to better understand the mechanisms related to enhancing adhesively bonded joints strength, this work aims to analyse the influence of different CFRP patterning layups on the fracture toughness of bonded joints and how the undergoing damage mechanisms can affect the crack propagation rate. Moreover, the Cohesive Zone Model (CZM) is used as a qualitative tool to understand the fracture mechanisms involved during Double Cantilever Beam (DCB) tests.

2. Materials and methods

2.1 Samples manufacturing

The Hexply 8552 – AS4, toughened epoxy resin supplied in prepreg unidirectional carbon fibres, was used to produce composites substrates with the following stacking sequences: $[0]_8$, $[0/90_2/0]_s$ and $[90/0_2/90]_s$. The curing of the composites laminated was performed in an autoclave under a total pressure of 7 bar and a temperature cycle of 180°C for 120 min.

Two different structural adhesives were used to join the CFRP substrates: a high toughness epoxy film adhesive with carrier 3M Scotch-weld™ AF163-2k (G_{IC} = 2416 J/m^2) [12] and a low toughness bi-component epoxy paste adhesive Araldite 2015/1 (G_{IC} = 640 J/m^2) [13], supplied by Hunstman International. The curing procedure for each adhesive is shown in Table 1.

Before the bonding procedure, the substrates' surfaces were sanded to ensure a uniform roughness, cleaned using acetone, and followed by a UV treatment for 7 minutes, as detailed in [12].

Each adhesive presented a different curing process, as described in Table 1.

Table 1: Description of adhesive's curing procedure.

Adhesive type	Temperature (°C)	Time (minutes)	Pressure (bar)	Method
Araldite 2015/1	80	60	-	Oven
AF- 163 2K	120	90	3	Autoclave

The dimensions of the CFRP adhesively bonded DCB specimens are detailed in Figure 1 (a). An initial crack length of 35 mm was guaranteed using Teflon tape. For AF163-2K, an inner carrier

ensured a nominal thickness of around 0.3 mm. For Araldite 2015/1, metallic spacers were used at both ends of the specimen to ensure the min thickness of 0.3 mm.

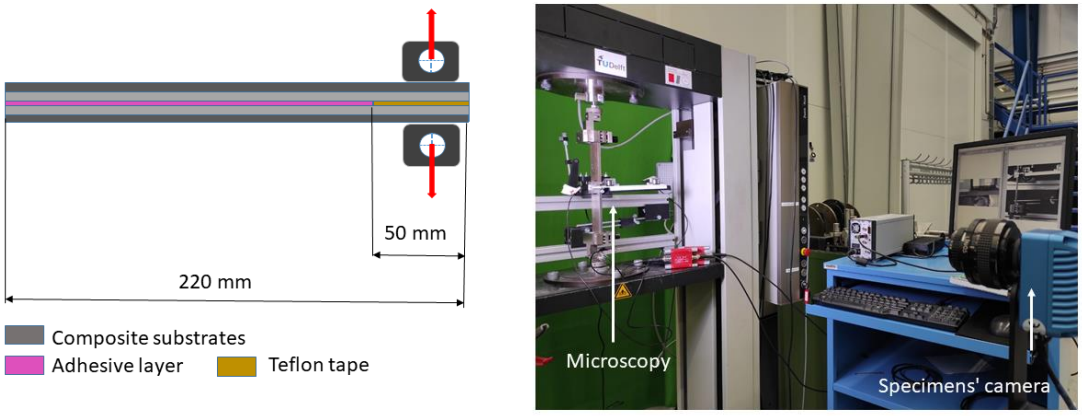

(a) (b)

Figure 1: (a) DCB dimensions and (b) testing set-up.

2.2 Experimental setup

DCB quasi-static mode I test were performed using an electro-mechanical Zwick testing machine with a Load cell of 1 kN. A testing speed of 4 mm/min was applied. At least four specimens of each type were tested, and their nomenclature is described in table 2.

Table 2: Specimens type and nomenclature.

Adhesive /CFRP layup	$[0]_8$	$[0/90_2/0]s$	$[0/90_2/0]s$
Araldite 2015/1	Araldite $[0]_8$	Araldite $[0/90_2/0]s$	Araldite $[0/90_2/0]s$
AF- 163 2K	AF – 163 2K $[0]_8$	AF – 163 2K $[0/90_2/0]s$	AF – 163 2K $[0/90_2/0]s$

Visual inspection was done on both lateral sides of the DCB specimens; on one side, using a microscope camera, and a regular camera on the other side, as shown in Figure 1(b). Both cameras were synchronised with load and displacement outputs from the testing machine. In addition, the photos were taken every four seconds.

The lateral surface used for regular camera photos was white painted to improve the contrast to track crack propagation. On the other side, the surface used for the microscopy camera measurements was kept natural to allow better visualisation of the crack path during the entire test.

  doi:10.5075/epfl-298799_978-2-9701614-0-0

3. Finite element analysis

Aiming to qualitatively simulate the crack propagation paths in the CFRP secondary bonded joints tested, a finite element model based on Cohesive Zone Modeling (CZM) was built.

A 3D finite element model for DCB specimens, under pure mode I, was set up in the ABAQUS software. In addition, a CZM with bi-linear traction separation law was applied. The substrates were modelled using eight-node brick elements (C3D8) and the cohesive elements with eight-node three—dimensional cohesive elements (COH3D8).

After a convergence study, a reasonable sweep mesh size of 0.5 mm was implemented for all the analyses.

To detect crack deflection and propagation in numerous possible paths, very thin cohesive element layers (5 microns thickness) were positioned at three different locations, as shown in Figure 2:

(1) in the middle of the adhesive layer to simulate cohesive failure.
(2) between each composite ply in a longitudinal direction to simulate delamination between composite plies.
(3) in the transversal direction next to the crack tip region to simulate transverse matrix cracking at the 90° lamina.

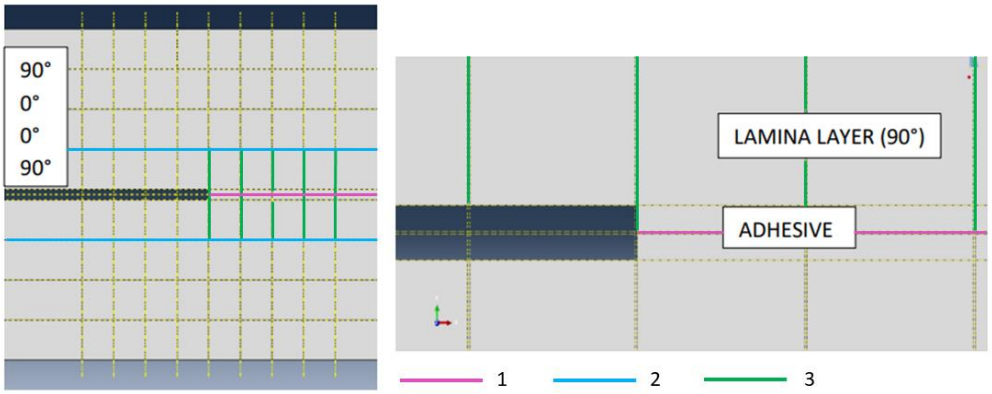

Figure 2: Scheme of the cohesive element layers distribution in the finite element analysis.

The distance between the cohesive element layers is equal to 0.375 mm. It is worth mentioning that each cohesive element layer had its properties correlated to the type of damage to be simulated represented (composite's matrix failure, delamination, or adhesive properties). The primary materials' properties used in the model are described in Tables 2 and 3.

  doi:10.5075/epfl-298799_978-2-9701614-0-0

Table 3: CZE properties used in cohesive interfaces of the FEA.

Material	E (MPa)	G (N/mm)	σ (MPa)
Araldite 2015/1	1.0E6	500	22
AF 163- 2K	1.0E6	2416	46
Hexply 8552 – AS4	1.0E6	500	64

Table 4: Composite material's properties used in the FEA.

Material	E_{11} (MPa)	E_{22} (MPa)	E_{33} (MPa)	V_{12} - V_{13}	V_{23}	G_{11} (MPa)	G_{22} (MPa)	G_{33} (MPa)
Hexply 8552 – AS4	141000	9750	9750	0.267	0.5	5200	5200	3190

4. Results

The load versus displacement curves of the DCB, and corresponding R-curves and fracture surfaces are shown in Figure 3. Moreover, specimens' onset fracture toughness and the crack onset location are presented in Table 4. The G_{IC} was calculated using the Corrected Beam Theory, as recommended by the standard ASTM D5528.

The specimens adhesively bonded with Araldite 2015/1 all showed cohesive failure independently of the substrates' layup ($[0]_{8,}$ $[0/90_2/0]$s and $[0/90_2/0]$s) and with maximum load values around 40-50N. The different stacking sequences did not affect the crack propagation paths, and no significant changes were observed in the onset fracture toughness. The average onset value of G_{IC} is around 600 J/m^2, and it is in accordance with the nominal fracture toughness of the Araldite 2015-1, which varies between 400 to 600 J/m^2.

On the other hand, specimens bonded with the film-adhesive AF 163- 2k showed different results depending on the substrates' stacking sequence. The $[0]_8$ layup showed a consistent cohesive crack propagation and an average onset fracture toughness of 2868 J/m^2. Moreover, an interesting bridging phenomenon triggered by the presence of the carrier inside the adhesive was observed [12]. This bridging phenomenon furtherly enhanced the adhesive's fracture toughness by around 20% as the crack further propagated along the specimen's lenght.

The specimens $[0/90_2/0]$s – AF163 – 2K showed a load versus displacement curves with a first peak that characterises the onset of damage without any visible crack, a 1st drop in the load values that corresponds to a matrix cracking at the 90-degrees ply (see Figure 4), a second peak related to a cohesive failure in the adhesive followed by a significant drop corresponding to delamination through the 0-degrees ply. In this case, it was possible to observe a crack competition between the initial cohesive failure and the matrix cracking. The last one promoted a crack deflection and final delamination at the 0-degree layer. Also, higher values of the joint's onset fracture toughness were obtained for these specimens compared to the $[0]_8$ with a total value of 3568 J/m^2 (25 % increase).

For specimens $[90/0_2/90]$ s – AF163 – 2K (Figure 3e), the crack onset deflected directly for the first 90-degree layer next to the adhesive layer, and a decrease in the joint's G_{IC} was obtained.

Through the numerical simulations, it was possible to observe that, for this specific case, the damage at the cohesive layer at the first composite layer next to the crack tip was significant and had a larger influence on the crack propagation path, as can be seen by the red colour (maximum degradation of the cohesive element) in Figure 4. Figure 3 (a) for this specimen also shows a non-smooth crack propagation, characterised by a stick-slip trend in the load-displacement curve that was not evident for the other specimens.

As shown in Table 4 and Figure 4, the finite element analysis could qualitatively predict the crack propagation paths in the specimens.

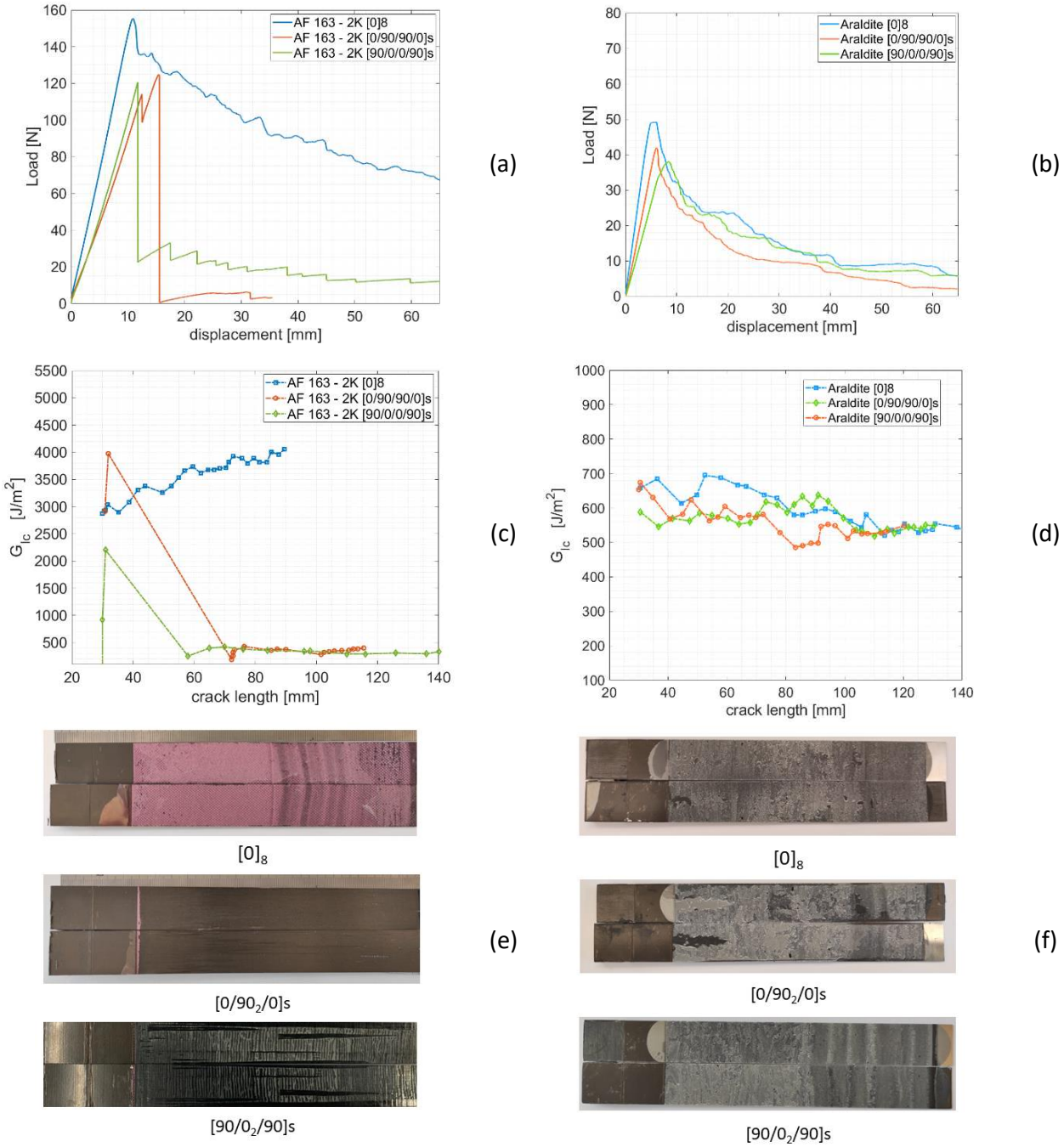

Figure 3:Load versus displacement curves (a) AF163-2K, (b) Araldite 2015/1, R- curves: (c) AF163-2K, (d) Araldite 2015/1, and fracture surfaces: (e) AF163-2k and (f) Araldite 2015-1.

Table 5: Mode I fracture toughness of each bunch of specimens and their crack onset observed experimentally and predicted by FEA.

Adhesive type	**CFRP stacking sequence**	**G_{IC} (J/m²) at crack onset**	**Crack onset** (experimental)	**Crack onset** (FEA)
AF 163 – 2K	$[0]_8$	2868	adhesive	-
	$[0/90_2/0]s$	3568	adhesive followed by matrix cracking	adhesive
	$[90/0_2/90]s$	2147	composite layup	Adhesive and composite layup
Araldite 2015-1	$[0]_8$	619.7	adhesive	-
	$[0/90_2/0]s$	563.9	adhesive	adhesive
	$[90/0_2/90]s$	600.1	adhesive	adhesive

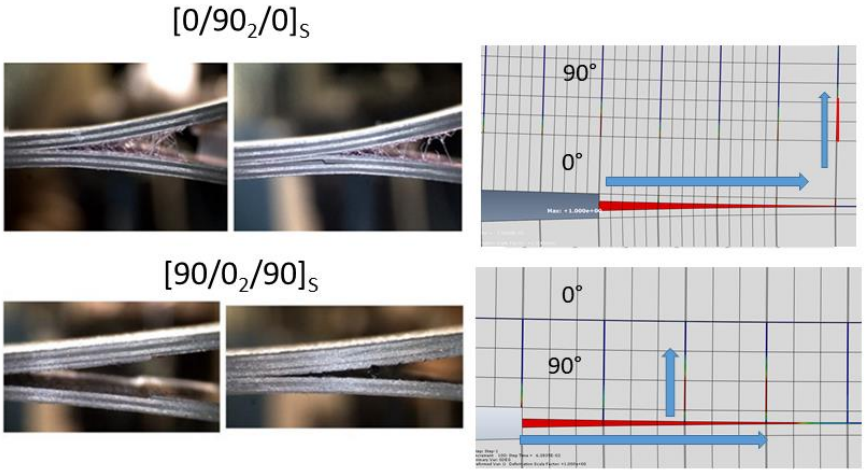

Figure 4: DCB specimens bonded with adhesive AF 163-2K with their crack paths visualised experimentally and by FEA.

5. Conclusions

This work studied the effects of CFRP layup patterning to enhance the secondary bonded joints' fracture toughness. The following conclusions could be drawn from the results:

  doi:10.5075/epfl-298799_978-2-9701614-0-0

When using a low toughness adhesive as the Araldite 2015/1 all fractures were cohesive, i.e., crack onset and propagations within the adhesive layer, indicating that the ultimate transverse strength of the CFRP plies was not exceeded. When using a high toughness adhesive as the AF 163-2K, , a crack competition was triggered between different crack locations (adhesive layer, matrix cracking, and delamination), influenced by different stress concentrations regions within the joint.

For the specimens bonded with the more tough adhesive, the CFRP patterning had a leading role in the G_{IC} of the studied joints. In particular, specimens $[0/90_2/0]s$ increased around 25% their onset fracture toughness compared to the unidirectional specimens. Moreover, the unidirectional specimens presented a bridging phenomenon triggered by an inner carrier that also lately enhanced their $G_{IC.}$ These results show promising solutions for enhancing the fracture toughness of mode I adhesively bonded joints.

Acknowledgements

This article/publication is based upon work from COST Action CA18120 (CERTBOND - https://certbond.eu/), supported by COST (European Cooperation in Science and Technology).

6. References

[1] M. D. Banea and L. F. M. Da Silva, “Adhesively bonded joints in composite materials: An overview,” *Proc. Inst. Mech. Eng. Part L J. Mater. Des. Appl.*, vol. 223, no. 1, pp. 1–18, 2009.

[2] M. Kadlec, R. Růžek, and P. Bělský, “Concurrent use of Z-pins for crack arrest and structural health monitoring in adhesive-bonded composite lap joints,” *Compos. Sci. Technol.*, vol. 188, no. December 2019, 2020.

[3] K. Maloney and N. Fleck, “Toughening strategies in adhesive joints,” *Int. J. Solids Struct.*, vol. 158, pp. 66–75, 2019.

[4] A. Buchman, H. Dodiuk-Kenig, A. Dotan, R. Tenne, and S. Kenig, “Toughening of Epoxy Adhesives by Nanoparticles,” *J. Adhes. Sci. Technol.*, vol. 23, no. 5, pp. 753–768, 2009.

[5] T. Kruse, T. Körwien, S. Heckner, and M. Geistbeck, “Bonding of CFRP primary aerospace structures - Crackstopping in composite bonded joints under fatigue,” *ICCM Int. Conf. Compos. Mater.*, vol. 2015-July, no. July, pp. 19–24, 2015.

[6] D. Quan, J. L. Urdániz, C. Rouge, and A. Ivanković, “The enhancement of adhesively-bonded aerospace-grade composite joints using steel fibres,” *Compos. Struct.*, vol. 198, pp. 11–18, Aug. 2018.

[7] R. Tao, X. Li, A. Yudhanto, M. Alfano, and G. Lubineau, “On controlling interfacial heterogeneity to trigger bridging in secondary bonded composite joints: An efficient strategy to introduce crack-arrest features,” *Compos. Sci. Technol.*, vol. 188, no. December 2019, p. 107964, 2020.

[8] R. Tao, X. Li, A. Yudhanto, M. Alfano, and G. Lubineau, “Laser-based interfacial patterning enables toughening of CFRP/epoxy joints through bridging of adhesive ligaments,” *Compos. Part A Appl. Sci. Manuf.*, vol. 139, no. September, p. 106094, 2020.

[9] S. Yin *et al.*, “Toughening mechanism of coelacanth-fish-inspired double-helicoidal composites,” *Compos. Sci. Technol.*, vol. 205, no. September 2020, p. 108650, 2021.

[10] J. Kupski, S. Teixeira de Freitas, D. Zarouchas, P. P. Camanho, and R. Benedictus, “Composite layup effect on the failure mechanism of single lap bonded joints,” *Compos. Struct.*, vol. 217, pp. 14–26, Jun. 2019.

[11] J. Kupski, D. Zarouchas, and S. Teixeira de Freitas, “Thin-plies in adhesively bonded carbon fiber reinforced polymers,” *Compos. Part B Eng.*, vol. 184, p. 107627, 2020.

[12] S. Teixeira de Freitas, D. Zarouchas, and J. A. Poulis, “The use of acoustic emission and composite peel tests to detect weak adhesion in composite structures,” *J. Adhes.*, vol. 94, no. 9, pp. 743–766, 2018.

[13] R. Lopes Fernandes, S. Teixeira de Freitas, M. K. Budzik, J. A. Poulis, and R. Benedictus, “From thin to extra-thick adhesive layer thicknesses: Fracture of bonded joints under mode I loading conditions,” *Eng. Fract. Mech.*, vol. 218, Sep. 2019.

